

## EULERIAN DESCRIPTION OF A STIRRED SUSPENSION USING TWO-PHASE POSITRON EMISSION PARTICLE TRACKING

Antonio Guida, Alvin W. Nienow, Mostafa Barigou\*

*School of Chemical Engineering, University of Birmingham, Edgbaston,  
Birmingham, B15 2TT, UK; \*Corresponding author: [m.barigou@bham.ac.uk](mailto:m.barigou@bham.ac.uk)*

**Abstract.** The technique of Positron Emission Particle Tracking (PEPT) is a unique non-intrusive Lagrangian flow visualisation technique which allows probing of opaque fluids and within opaque apparatus. It uses a single positron-emitting particle as flow tracer which is tracked in 3D space and time to reveal its full Lagrangian trajectory. PEPT was used to study the mixing of a concentrated suspension of coarse glass particles in a vessel agitated by a pitched blade turbine operating in both up-pumping and down-pumping modes. The Lagrangian information obtained was used to obtain a detailed Eulerian description of the two-phase flow inside the vessel. For the first time, it has been possible to determine the full 3D velocity and concentration fields of both the liquid and the solid phase within an opaque flow of this type.

**Keywords:** Mixing; PBT impeller; PEPT; suspension; two-phase flow.

### 1. INTRODUCTION

The suspension of solids in stirred vessels is ubiquitous in industry including the manufacture of fine chemicals, pharmaceuticals, personal/home care products, paper and pulp, polymers, food. Numerous difficult mixing problems are found with solid-liquid processing, some 80 % of products in the chemical industry, for example, being of this type. The methods generally used for designing stirred vessels for solid-liquid mixing tend to be based on a global 'black-box' approach, and a more detailed description of the internal flow structure is needed to aid the development of rational design rules. A localized hydrodynamic approach provides a better basis for design since it enables a detailed description of the multiphase flow structure to be obtained. Whereas for translucent systems Eulerian data have been available through the use of well established techniques such as LDV and PIV, these optical instruments, however, have only been applied to very dilute suspensions and cannot be applied to high concentration slurries which are opaque. So far, other attempts at local measurements have been mainly limited to the investigation of mean axial solid-concentration profiles at relatively low concentrations using intrusive conductivity or capacitance probes [1]. However, these methods give limited information and cannot be used to probe concentrated suspensions in detail or to measure the 3D distribution of both liquid and solid.

We report here on the use of the technique of Positron Emission Particle Tracking (PEPT) to study the mixing of a concentrated suspension of glass particles in water with concentrations varying up to 22.3 wt%. Detailed information is obtained on particle and fluid trajectories, two-phase flow field, and spatial distribution of both the liquid and solid phases.

## 2. EXPERIMENTAL

### 2.1. Positron Emission Particle Tracking

The technique of Positron Emission Particle tracking primarily involves the use of a radioactively labelled tracer particle, a positron camera and a location algorithm for computing the tracer location [2-4]. The tracer particle is labelled with a positron-emitting nuclide and the radio isotopes usually used are  $^{18}\text{F}$ ,  $^{61}\text{Cu}$  and  $^{66}\text{Ga}$ . A positron emitted by the particle tracer rapidly annihilates with an electron emitting a pair of almost collinear 511 keV  $\gamma$ -quanta in opposite directions. The detection in coincidence of these two  $\gamma$ -rays is the first step in locating the tracer by the positron camera. The camera consists of two  $\gamma$ -camera heads working in coincidence. When a positron annihilation occurs the  $\gamma$ -rays emitted produce two coincident scintillations in the crystals, the related photomultipliers generate positional signals and two 2D centroids are calculated by the software. The joining line is the photon-trajectory related to the annihilation event. With a small number of annihilation events (theoretically only two) the position of a single positron-emitting particle can be located at the intersection of the photon trajectories. The location algorithm calculates the time-space location of the radioactive tracer whilst discarding corrupt events.

### 2.2. Mixing vessel and solid-liquid suspension

PEPT experiments were conducted in a flat-base cylindrical vessel of diameter  $T = 288$  mm made of Perspex, as shown in Figure 1. The vessel was fitted with four wall baffles and was agitated by a 6-blade  $45^\circ$  pitched-turbine (PBT) of diameter  $D = 0.5T$ . The off-bottom clearance of the PBT was  $0.25T$ , and the height of the suspension was set at  $H = T$ . The suspending liquid used was an aqueous solution of NaCl of density  $1150 \text{ kg m}^{-3}$ . Nearly-monomodal and nearly-spherical glass beads ( $d = 2.85\text{-}3.30$  mm) having a density of  $2485 \text{ kg m}^{-3}$  were used to make a two-phase slurry with a mean solid mass concentration,  $X$ , varying in the range 5.2 to 22.3 wt%.

### 2.3. Selective radioactive labelling

PEPT experiments consisted of separately resolving the full three-dimensional trajectories of the fluid and of the solid particles in two successive and distinct experiments. A representative glass particle radioactively labelled with  $^{18}\text{F}$  was used to track the solid phase, whilst a neutrally-buoyant resin tracer of  $600 \mu\text{m}$  diameter also labelled with  $^{18}\text{F}$  was used to track the liquid phase. The theoretical premise which guarantees that a tracer is representative of all the solid or liquid phase is referred to as ergodicity or iso-probability condition. In a single phase system, such a condition implies an equal probability of tracer presence at every point in the flow. In a multiphase system, however, an equal total probability is required, i.e. the sum of probabilities of presence for all components of the system must be the same everywhere. Ergodicity is a theoretical state which can be approached only after an infinite tracking time. However, it can be mathematically shown that, if the probability of visits is sufficiently high everywhere, ergodicity can be safely assumed when the trajectory of the tracer is recorded over a sufficiently long time to achieve adequate data resolution in every region [5]. The PEPT tracking time in this study was set at 30 min for each phase, which was long enough to acquire sufficient data in all regions of the vessel. Hence, ergodicity could be safely assumed given that in such a system the probability of visits is sufficiently uniform because of the geometry of the vessel and high turbulence state of the slurry. Experiments were conducted at the minimum rotational speed for particle suspension,  $N_{js}$ , determined experimentally according to the well-known Zwietering criterion. Mixing of the suspension was investigated with the impeller pumping downwards (PBD) and upwards (PBU).

### 3. THEORY AND DATA ANALYSIS CODE

#### 3.1. Geometric efficiency

The flow field in a mixing vessel is very complex and is characterised by high local velocity gradients. For a constant frequency of acquisition of the 3D locations of the positron-emitting tracer, an acceleration of the tracer creates a dilation of the curvilinear distance separating two consecutively detected locations along the trajectory. Therefore, in the presence of a high velocity the density of tracer detections along the trajectory is reduced, which leads to an underestimation of the local velocity by virtue of the error incurred in linearly interpolating between two consecutive locations. This error is position dependent and, consequently, the region around the impeller which exhibits the highest local velocities should be affected by the highest underestimation error. However, the frequency of data acquisition is not constant and is dependent on the radioactivity of the tracer which decreases exponentially with time, and the probability of its detection which varies with its 3D location. Figure 2 is a two-dimensional illustration of how the location of the tracer can affect the probability of detection; to be detected, the two back-to-back  $\gamma$ -rays must travel inside the coloured area.

The probability of tracer detection can be assumed – to a first approximation – to be proportional to the geometric efficiency of detection which can be calculated through geometric considerations. Such an approximation is reasonable since other factors affecting the accuracy of PEPT (or their variation with location) are of a secondary order compared to the geometric efficiency (or its variation with location), including the possibility that two decay events may occur in the same time window, the range of the positron in the matter, the fact that the  $\gamma$ -rays are not exactly  $180^\circ$  apart ( $\pm 0.5^\circ$ ), photon absorption/scattering phenomena and the angle at which the  $\gamma$ -rays pass through the crystal inside the detector.

The infinitesimal probability that one  $\gamma$ -ray will travel inside the solid angle,  $d\Omega$ , subtended at the source by an infinitesimal area of a detector can be expressed by normalising this angle by the total solid angle ( $4\pi$ ). Considering that two  $\gamma$ -rays are emitted, the infinitesimal probability,  $dE_G$ , that one of the two photons will travel inside  $d\Omega$  can then be written as:

$$dE_G = 2 \frac{d\Omega}{4\pi} \quad (1)$$

After double integration, it can be shown that the geometric efficiency,  $E_G$ , assumed to be proportional to the probability of detection, is a function of the following variables:

$$E_G = E_G(x, y, z, L_D, H_D, S_D) \quad (2)$$

The above function becomes a 3D-function (only position dependent), for given dimensions  $L_D$  and  $H_D$  of the rectangular active area of the  $\gamma$ -ray detectors, and a fixed separation  $S_D$  between them. Note that whilst  $L_D$  and  $H_D$  are fixed by the size of the detectors' active area

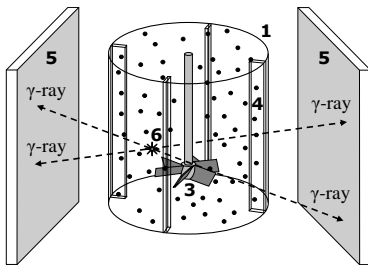


**Figure 1.** Experimental PEPT set-up: 1 cylindrical tank; 2 shaft; 3 PBT; 4 baffle; 5  $\gamma$ -ray detectors; 6 particle tracer.

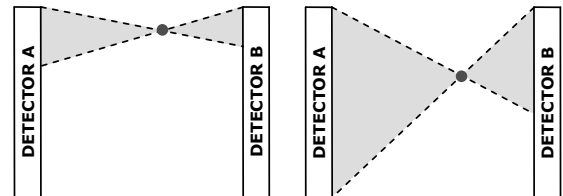


**Figure 2.** 2D illustration of the effect of the angle subtended at the source by both detectors on the geometric efficiency.

( $470 \times 590 \text{ mm}^2$ ),  $S_D$  can be varied up to a maximum of 800 mm to suit the size of the flow system under investigation. Two-dimensional maps of the geometric efficiency are depicted in Figure 3 at selected heights within the detection space for a value of  $S_D$  equal to 400 mm.  $E_G$  is maximum at the origin of coordinates, i.e. at the centre of the detection space, and is zero at the edges. Consequently, the probability and, hence, the number of successfully detected positions of a particle tracer, tends to be highest in the centre between the detectors.

As pointed out above, in a stirred vessel the central region should be affected most by an underestimation of tracer velocity due to the high local velocities, but at the same time the probability of detection there is the highest. On the other hand, near the wall of the tank the velocities are smaller but the probability of detection is lower. Consequently, these two effects tend to approximately cancel each other for an accurately centred tank with dimensions not too close to those of the detectors and, given that  $H_D > L_D$ , a separation  $S_D$  chosen so that  $H_D > S_D > L_D$  and the detection space is approximately cubical.

### 3.2. Eulerian maps

A new code was developed to analyse PEPT flow data which calculates Lagrangian velocities along the trajectory of the tracer using the Least Squares Method. The code allows the user to define the number of successive positions used in determining the tracer velocity according to the flow regime considered. These velocities are then converted to Eulerian velocities using a 3D user-defined grid consisting of a large number of equal volume cells,  $N_C$ . In a given cell, the code determines the mean velocity components,  $u_r$ ,  $u_\vartheta$ ,  $u_z$ , along the segment of trajectory intersecting with the cell in each visit, and averages again by the number of visits. A number of other local quantities are determined within each cell including Eulerian maps of the magnitude of the total 3D-velocity and of the 2D radial-axial velocity, standard deviation of the velocity components and of the total velocities (2D and 3D), tracer acceleration, number of PEPT tracer locations, probability of tracer presence and frequency of visits.

### 3.3. PEPT locations filter

A basic step in the analysis of PEPT data is the elimination of the occasionally corrupt locations not discarded by the initial PEPT reconstruction algorithm, which may be caused by spurious radioactivity from the surroundings. A filter function has been developed to efficiently remove such corrupt locations. The filter operates locally taking into account the geometric efficiency, local flow velocity, and decreasing residual radioactivity of the tracer.

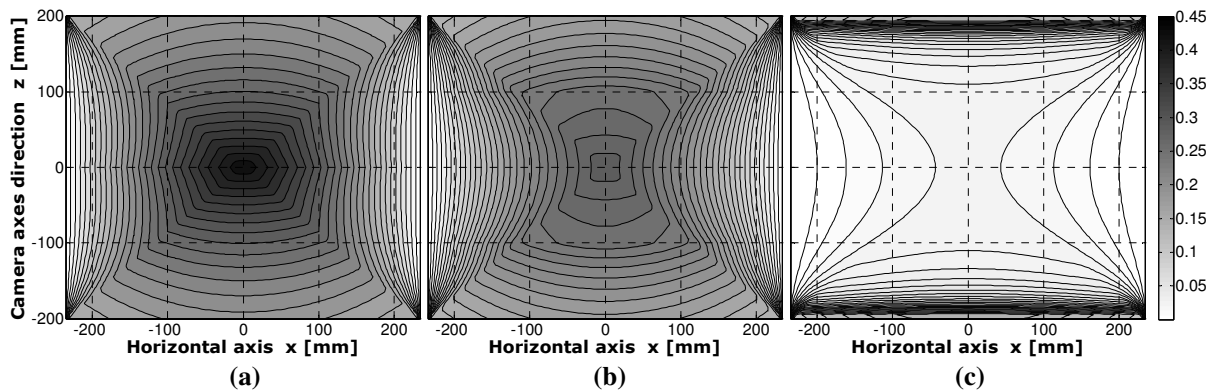


**Figure 3.** Two-dimensional horizontal maps of geometric efficiency,  $E_G$ , with the origin of coordinates placed in the centre of the detection space and detector separation  $S_D = 400$  mm: (a) middle plane,  $y = 0$  mm; (b) plane at  $y = \pm 150$  mm; (c) plane near the upper/lower limit of the detection space,  $y = \pm 285$  mm.

### 3.4. Dummy locations

Another fundamental aspect of PEPT data analysis is dealing with the occasional short interruptions in the trajectory caused by incidents of low frequency of data acquisition, as discussed above. The effect of such short trajectory interruptions is negligible when the velocity is low, but cannot be ignored when the tracer is moving at a high velocity. Where there are interruptions in the tracking of the tracer, it is not usually possible to know where the tracer has been during this interruption time, but it is possible as a first approximation to define a linear segment of trajectory between the last and the next detected location, which assumes that the tracer moves at a constant velocity between the two points. Thus, a dummy location or ghost point is inserted in the middle between two consecutive intersections within the defined grid, i.e. inside each cell. This operation should improve the measurement accuracy of the time the tracer spends in each cell, but the effect on the calculated velocity field is not expected to be significant unless the rate at which tracking is interrupted is high.

### 3.5. Spatial phase distribution

In addition to location and velocity information, PEPT allows the particle-tracer occupancy distribution within the vessel to be computed, which offers an additional powerful tool for characterising flow behaviour within the mixing tank. Occupancy has usually been obtained by calculating the fraction of the total experimental time,  $t_\infty$ , spent by the tracer in each cell during the experiment. Such a definition establishes a mathematical identity between occupancy and probability of presence of the particle tracer but makes occupancy highly dependent on the density of the grid, so that as the number of cells increases occupancy tends to zero. If the cells are chosen to have equal volume, however, using the ergodic time defined as  $t_E = t_\infty / N_C$  instead of the total experimental time circumvents this problem; this represents the time that the tracer would spend in any cell if the flow were single phase and ergodic. This definition makes it then possible to describe the spatial distribution of each phase component within a multiphase flow.

The infinitesimal probability that a specific solid particle is inside an infinitesimal volume element  $dV$  is a function of the particle position  $\mathbf{P}$  and can be expressed from two different points of view. From the Lagrangian point of view, it is the ratio of the infinitesimal time  $dt$  that the tracer spends inside  $dV$ , to the total time of detection  $t_\infty$ ; in Eulerian terms, however, it is the ratio of the number of solid particles  $dn$ , contained in  $dV$ , to the total number of such particles in the vessel  $n$ . Thus, it follows that:

$$f(\mathbf{P})dV = \frac{dt}{t_\infty} \quad \text{and} \quad f(\mathbf{P})dV = \frac{dn}{n} \quad \Rightarrow \quad \frac{dt}{t_\infty} = \frac{dn}{n} \quad (3)$$

Introducing the volume of a single particle  $V_p$ , the infinitesimal solid volume  $dV_S$  in  $dV$ , the total solid volume present in the tank  $V_S$ , the local volume concentration  $C$ , the mean volume concentration  $\langle C \rangle$ , and the total volume of the multiphase suspension  $V_T$ , yields:

$$\frac{dt}{t_\infty} = \frac{dn}{n} = \frac{V_p dn}{V_p n} = \frac{dV_S}{V_S} = \frac{CdV}{\langle C \rangle V_T} \quad (4)$$

If the cell volume,  $\Delta V$ , is uniform, the total number of grid cells is  $N_C = V_T / \Delta V$ , and rewriting the above equation in discrete terms leads to:

$$\frac{\Delta t}{t_\infty} = \frac{C\Delta V}{\langle C \rangle V_T} \quad \Rightarrow \quad \frac{\Delta t}{t_E} = \frac{N_C \Delta t}{t_\infty} = \frac{C}{\langle C \rangle} \quad (5)$$

Defining, as discussed above, the occupancy as the ratio of time that the tracer spends inside a

cell to the ergodic time, Eq. (5) then becomes:

$$O_E = \frac{C}{\langle C \rangle} \quad (6)$$

Note that it can be readily shown that Eq. (6) is also valid in the case of a fluid component. The direct important consequence of Eq. (6) is that it is now possible to fully map by PEPT the local concentration of each component (solid and liquid) in an opaque multiphase system.

#### 4. RESULTS AND DISCUSSION

The data analysis was conducted using the newly developed code described above, and some sample maps of the velocity field and phase concentration profiles are shown in Figure 4. Using cylindrical coordinates, the radial-axial 2D velocity maps were obtained by azimuthally averaging the 3D velocity data and projecting them onto the 2D radial-axial plane. A similar averaging process was used to obtain the radial concentration profiles in Figure 4e. The velocity plots shown are normalised with the impeller tip speed,  $u_{tip}$ . The observed flow field with a single flow loop is typical of a down-pumping PBT, whilst an up-pumping PBT usually gives rise to a double flow loop. As expected, particle velocities are relatively high in the impeller region and around the centre of the flow loops but low in the upper parts of the tank and in the centre of the loops. Data available in the literature for single-phase systems show similar features. As a consequence, a comparison of liquid flow maps under single-phase flow conditions and in the presence of a solid phase should lead to qualitative similarities. PEPT experiments conducted at the same rotational speed with a single-phase solution confirmed these similarities. In order to further assess the effect of the presence of solid particles on the flow field of the liquid phase, the flow number was estimated. The volumetric flow rate,  $Q$ , of fluid discharged by the agitator was determined at the horizontal edge of the blades by integrating the axial velocity profile in the impeller discharge, and the dimensionless flow number was computed, thus:

$$Fl = \frac{Q}{ND^3} = \frac{1}{ND^3} \int_{PBT} u_z dS \quad (7)$$

where the integral was evaluated over the discharge section of the impeller (upper for PBTU

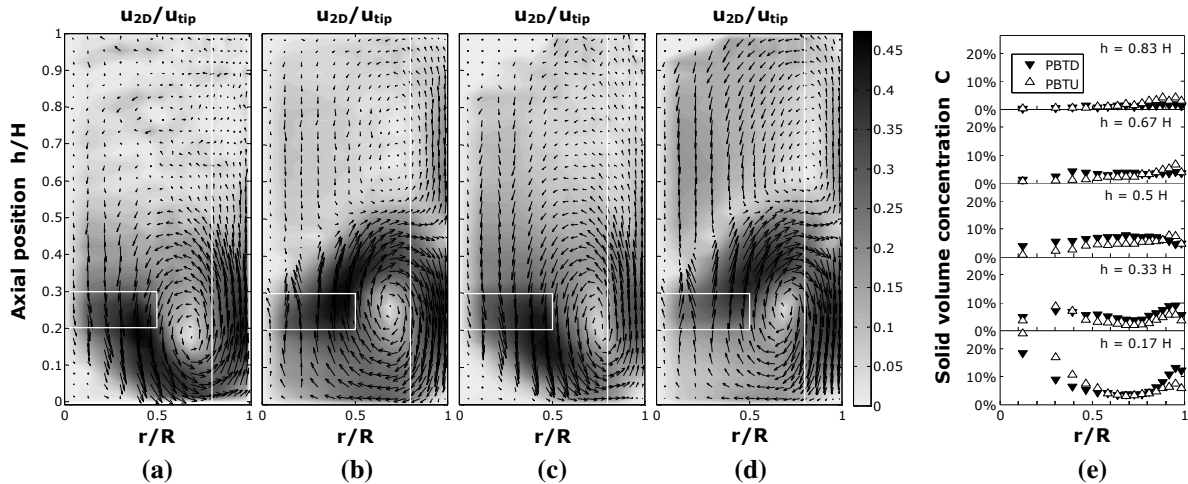


**Figure 4.** Azimuthally-averaged radial-axial velocity maps,  $\langle C \rangle = 5.2 \text{ vol}\%$  ( $X = 10.6 \text{ wt}\%$ ): (a) liquid, PBT; (b) liquid, PBTU; (c) solid, PBT; (d) solid, PBTU. Azimuthally-averaged volume concentration radial profiles,  $\langle C \rangle = 5.2 \text{ vol}\%$  ( $X = 10.6 \text{ wt}\%$ ): (e) solid PBTU/PBT.

and lower for PBTD). As shown in Figure 5, the presence of the solid phase seems to cause only a small reduction in  $Fl$  which diminishes even further as  $N$  increases above  $N_{js}$ . However, it should be noted that these results relate to a fairly moderate solid concentration ( $X = 5.2$  wt%), and the effects may be more pronounced at higher concentrations.

The vertical profiles of the volume concentration of the solid phase, averaged azimuthally and radially are displayed in Figure 6 for different solid concentrations. The plots show the high degree of vertical non-uniformity of the suspension, with a minimum at the impeller level and a maximum above it, near the central plane. The shape of the plots shows a good qualitative agreement with one-dimensional data for a different system available in the literature, obtained by slurry sampling at the wall [6]. The PEPT results presented here, however, are much more detailed as local values are determined everywhere in the vessel, which has not been possible before with sampling or probe methods.

The substantial variation of the local solid concentration with location in the vessel, as demonstrated by the radial distributions in Figure 4e and the axial profiles in Figure 6, justifies the introduction of a global uniformity index,  $\zeta$ , to enable a quantitative description of the degree of uniformity of the distribution, thus:

$$\zeta = \frac{1}{\sigma^2 + 1} = \frac{1}{\frac{1}{N_C} \sum_{i=1}^{N_C} \left( \frac{C_i - \langle C \rangle}{\langle C \rangle} \right)^2 + 1} = \frac{\langle C \rangle^2}{\langle C^2 \rangle} \quad (8)$$

where  $i$  is the cell number within the measurement grid. The index is conveniently defined so

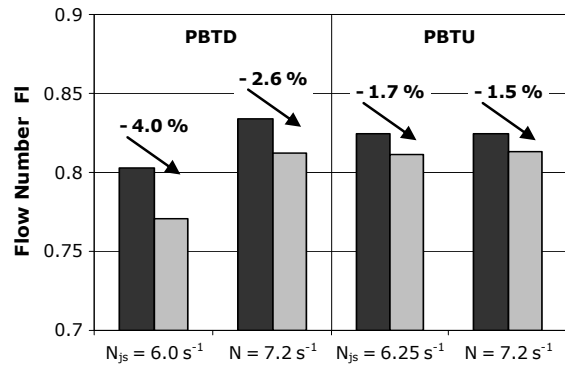


Figure 5. Effect of the presence of the solid phase on  $Fl$ : ■  $X = 0$  wt%; □  $X = 5.2$  wt%.

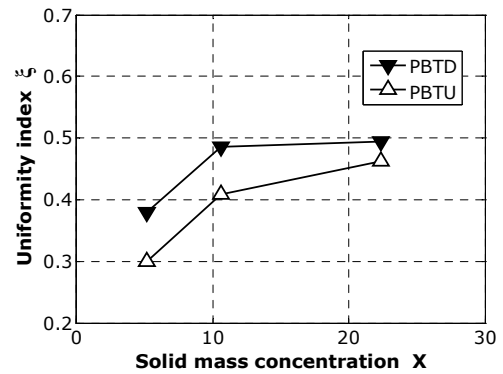


Figure 7. Variation of the uniformity index  $\zeta$  as a function of total solid concentration.

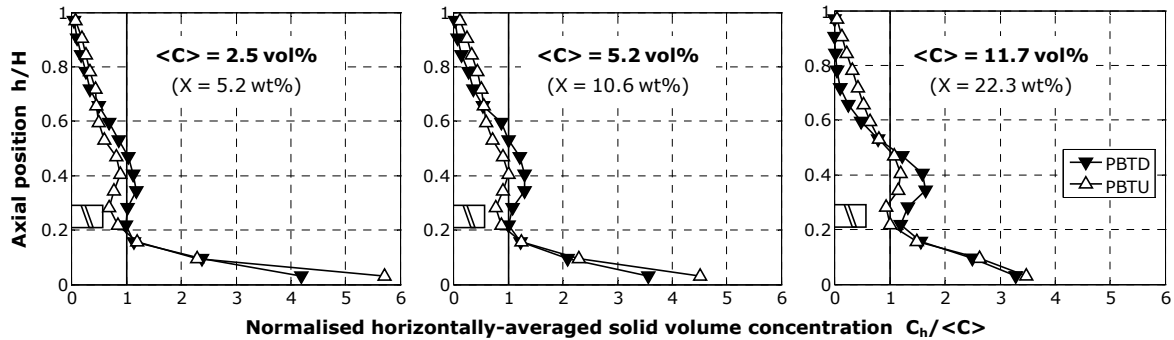


Figure 6. Vertical normalised profiles of azimuthally and radially-averaged solid volume concentration.

that as  $\zeta \rightarrow 0$  the uniformity of the suspension is at its minimum (condition achieved for a theoretically infinite variance,  $\sigma^2$ , of the normalised local concentration); and when  $\zeta = 1$  the solids are uniformly distributed within the vessel volume, i.e. there are no solid concentration gradients present and the total solid concentration is equal to the average concentration in the vessel (i.e.  $\sigma^2 = 0$ ). The variation of the index  $\zeta$  as a function of average mass concentration  $X$  is represented in Figure 7, for both the up-pumping and down-pumping PBT. The results show that  $\zeta$  increases with  $X$  for both modes of impeller operation. For a given solid concentration, a PBTD achieves a more uniform suspension compared to a PBTU, but the difference between the two pumping modes becomes small at high solid concentrations.

Furthermore, the pointwise measurements obtained with PEPT have now enabled, for the first time, the solids mass balance throughout the vessel and the mass continuity of the two phases to be accurately verified, so that:

$$\frac{1}{N_H} \sum_{j=1}^{N_H} C_h^{(j)} = \langle C \rangle \quad \text{and} \quad \sum_S \mathbf{u} \cdot \Delta \mathbf{S} \cong 0 \quad (9)$$

where  $S$  is a closed surface. Calculations were made considering a cylinder with the same vertical axis, base and diameter as the tank but with a shorter height and a closed surface  $S$  as indicated in Eq. (9). Because of  $\mathbf{u}$  the term  $\mathbf{u} \cdot \Delta \mathbf{S}$  is zero everywhere except in the horizontal plane across the tank, so that  $S$  can be coincided with such a plane. Dividing the vessel into equal volume cells makes  $|\Delta \mathbf{S}|$  a constant, which reduces Eq. (9) to a zero sum (or average) of axial velocities across the horizontal plane considered. For the PEPT velocity fields, calculations gave a velocity average close to zero, i.e.  $< 0.02u_{tip}$ .

## 5. CONCLUSIONS

PEPT is a powerful non-invasive technique which is ideally suited to the study of opaque multiphase systems. For the first time, it has been possible to determine the trajectory, the full 3D velocity field and spatial distribution of both the liquid and the solid phase within an opaque concentrated suspension. The technique can now be extended to the study of more complex polydisperse systems. Such unique data are invaluable both in their own right and for the validation of numerical codes, and should help unravel some of the unsolved problems in the field of solid-liquid mixing.

## 6. REFERENCES

1. Brunazzi E., Galletti C., Paglianti A., Pintus S., 2004. "An Impedance Probe for the Measurements of Flow Characteristics and Mixing Properties in Stirred Slurry Reactors", *Chem Eng Res Des*, **82**(A9), 1250-1257.
2. Barigou M., 2004. "Particle tracking in opaque mixing systems: An overview of the capabilities of PET and PEPT", *Chem Eng Res Des*, **82**(A9), 1258-1267.
3. Parker D.J., Forster R.N., Fowles P., Takhar P.S., 2002. "Positron emission particle tracking using the new Birmingham positron camera", *Nucl Instrum Meth A*, **477**(1-3), 540-545.
4. Fangary Y.S., Barigou M., Seville J.P.K., Parker D.J., 2002. "A Lagrangian study of solids suspension in a stirred vessel by Positron Emission Particle Tracking (PEPT)", *Chem Eng Technol*, **25**(5), 521-528.
5. Wittmer S., Falk L., Pitiot P., Vivier H., 1998. "Characterization of stirred vessel hydrodynamics by three dimensional trajectory", *Can J Chem Eng*, **76**(3), 600-610.
6. Barresi A., Baldi G., 1987. "Solid dispersion in an agitated vessel", *Chem Eng Sci*, **42**(12), 2949-2956.